

Agata Merda, Grzegorz Golański, Paweł Wieczorek, Kamil Staszalek

## The Analysis of the Microstructure of Welded Joints in Steel P5 after Service

**Abstract:** The material subjected to the tests discussed in the article was a section of a welded joint made of bainitic steel P5. The joint subjected to analysis was sampled from a pipe section exposed to the effect of elevated temperature for more than 96 000 hours. The metallurgical tests revealed a relatively low degree of the degradation of the test joint. The microstructure contained retained bainite and precipitates of various morphology. The identification of precipitates revealed the presence of  $M_{23}C_6$  and  $M_2C$  precipitates in the joint. The  $M_{23}C_6$  carbides were observed along the boundaries of former austenite grains. The above-named identification of precipitates also revealed the presence of  $M_2C$  and  $M_{23}C_6$  carbides within the grains/laths. The insignificant exhaustion of the joint microstructure might be ascribed to the fact that the joint was subjected to relatively low temperature for a relatively short time.

**Keywords:** welded joint, steel P5, microstructure

**DOI:** [10.17729/ebis.2020.5/1](https://doi.org/10.17729/ebis.2020.5/1)

### Introduction

High-temperature creep resistant materials presently used in the power engineering sector have to be characterised by the stable microstructure and properties ensuring the safe operation of power units for a minimum of 200 000 hours. The initial assessment of the suitability of a given alloy grade is performed under laboratory conditions, whereas its actual verification is carried out in industrial conditions [1– 3]. Metallurgical tests involving sections sampled from power generation systems aim

to assess the effect of operating parameters on the exhaustion of the microstructure and the reduced ability of the material to transfer actual service loads. The aforesaid tests not only enable the verification of the usability of a given material grade but also make it possible to build a material database. Another important issue concerning the assessment of the service life of power system structural elements is the evaluation of the service life of welded joints [4–7].

Bainitic steel P5 (designation in accordance with PN-EN X11CrMo5) has been developed in

---

mgr inż. Agata Merda (MSc Eng.), dr hab. inż. Grzegorz Golański (PhD (DSc) Habilitated), Professor at PCz; dr inż. Paweł Wieczorek (PhD (DSc) Eng.) – Częstochowa University of Technology; Institute of Materials Engineering; mgr inż. Kamil Staszalek (MSc Eng.) – „Pro Novum” Sp. z o. o. Science and Technology Service Company

Table 1. Chemical composition of steel P5, % by weight [9]

	C	Si	Mn	P	S	Cr	Mo
Min	0.008	0.25	0.30	-	-	4.00	0.45
Max	0.25	0.50	0.60	0.025	0.01	6.00	0.65

the United States of America and is used primarily to make pipelines applied in the petrochemical and power generation industries [8]. Steel P5 belongs to the groups of Cr-Mo steels, the required chemical composition of which is presented in Table 1. In comparison with “classical” low-alloy Cr-Mo steels, i.e. steel 10CrMo9-10 (10H2M) or steel 13CrMo4-5 (15HM), steel P5 (having a molybdenum content comparable to that of the classical chromium-molybdenum steels) is characterised by a higher chromium content (between 4% and 6%). If compared with low-alloy Cr-Mo steels, the higher content of chromium makes steel P5 more resistant to the effect of hydrogen sulphide and petroleum derivatives. In addition, the higher content of chromium increases high-temperature creep resistance and steel hardenability. In turn, the addition of molybdenum significantly increases creep resistance, prevents tempering brittleness and increases the corrosion resistance of chromium steels in reducing environments and environments containing chlorides. Molybdenum also increases the high-temperature creep resistance and the hardenability of steel.

Table 2. Parameters of heat treatment in relation to steel P5 [9]

Steel grade	Normalising temperature [°C]	Tempering temperature [°C]
P5 + NT1	930–980	730–770
P5+ NT2	930–980	710–750

The higher hardenability of steel P5 in comparison with that of low-alloy Cr-Mo steels enables the obtainment of the bainitic structure after cooling in air, whereas the wide tempering temperature range enables the obtainment required functional properties. The heat treatment of steel P5 is performed at two stages and involves normalising performed at a temperature restricted within the range of 930°C to 980°C followed by high-temperature hardening performed at temperature exceeding 700°C (Table 2). The mechanical properties of steel P5 required at room temperature are presented in Table 3.

The objective of the tests performed within the research work was to analyse the microstructure of steel P5 after more than 96 000 hours of operation at a temperature of 519°C.

### Testing methodology

The specimen subjected to the metallographic tests was a joint sampled from a section of a pipe (having an external diameter of 220 mm and a wall thickness of 9.1 mm) made of bainitic steel P5. The test joint was exposed to a temperature of 519°C and a pressure of 1.8 MPa for 96 000 hours. The scope of the tests included the following:

- analysis of the chemical composition of the base material and that of the filler metal, performed using a SpectroLab spark spectrometer,

Table 3. Mechanical properties required of steel P5 [9]

Steel grade	Tensile strength $R_m$ [MPa]	Upper yield point $R_{ch}$ or conventional yield point $R_{p0.2}$ in relation to wall thickness $T$ [MPa]				Elongation A [%]		Impact energy $KV_2$ [J]	
		$T \leq 16$	$16 < T \leq 40$	$40 < T \leq 60$	$60 < T \leq 100$	L	T	L	T
P5 + NT1	480–640	280	280	280	280	20	18	40	27
P5 + NT2	570–740	390	390	390	390	18	16	40	27

L – longitudinal, T – transverse

- macroscopic tests involving the cross-section of the welded joint, performed using an Olympus SZ61 light microscope;
- microstructural tests performed using an Axiovert 25 light microscope and an SEM Jeol JSM6610LV scanning electrode microscope. The test joint was subjected to etching in Nital. The size of former austenite grains was revealed by etching the specimen in the solution of picric acid;
- thermodynamic analysis performed using a ThermoCalc for Windows software programme (TCW);
- identification of precipitates performed using a JEM-2100 PLUS transmission electron microscope and selective microscopic diffraction.

The chemical composition of the base material is presented in Table 4. The analysis results confirmed that the chemical composition of the material corresponded to that of steel grade X11CrMo5 (P5) – Table 1. Table 5 presents the chemical composition of the weld, corresponding to that of filler metal Union I CrMo910.

Table 4. Chemical composition of steel P5, % by weight

C	Si	Mn	P	S	Cr	Mo
0.06	0.31	0.33	0.005	0.020	4.61	0.44

Table 5. Chemical composition of the weld, % by weight

C	Si	Mn	Cr	Mo
0.10	0.40	0.50	5.50	0.60

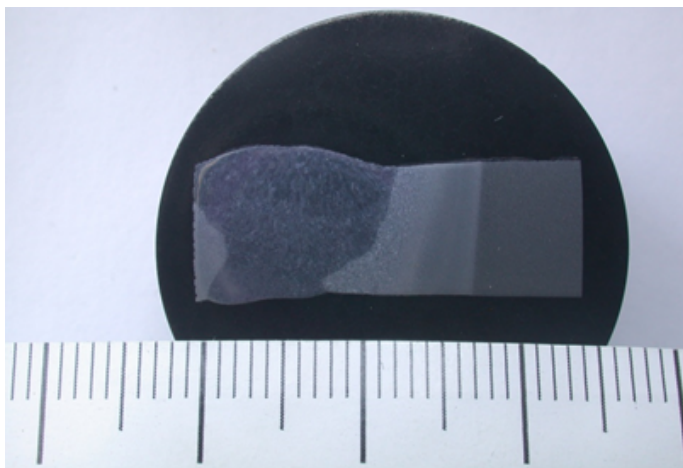


Fig. 1. Macroscopic image of the welded joint subjected to analysis

### Macroscopic tests

The macroscopic image of the welded joint subjected to analysis is presented in Figure 1. The cross-sectional observations revealed the proper structure of the joint. The joint did not contain any welding imperfections inconsistent with quality level B in accordance with the standard referred to in publication [10].

### Microscopic tests

#### Microstructure of the base material

The microstructural analysis of the test joint involved the base material, heat affected zone (HAZ) and the weld. In the as-received state, steel 5Cr-0.5Mo was characterised by the bainitic microstructure with lower bainite, granular bainite and single  $M_3C$  precipitates along former austenite boundaries and within bainite laths. In turn, the grains contained fine  $M_2C$  carbides [12, 13]. After the operation of previously specified duration, the microstructure in the base material area remained bainitic (with numerous precipitates) (Fig. 2).

The degree of the decomposition of the bainitic areas was relatively low. Precipitates of various morphology were observed within and on the boundaries of bainite laths as well as on the boundaries of former austenite grains. Depending on the chemical composition and the parameters of heat treatment, the microstructure of the Cr-Mo low-alloy steels in the as-received state contained  $M_3C$ ,  $M_7C_3$ ,  $M_{23}C_6$  and  $M_2C$  precipitates [11, 12]. The  $M_7C_3$  and  $M_{23}C_6$  precipitates were rich in chromium, the  $M_2C$  carbide was a precipitate rich in molybdenum, whereas the  $M_3C$  precipitates were alloy cementite [14]. The operation of Cr-Mo steel led to the evolution of the morphology of the carbides, i.e. the change of their chemical composition, coagulation, spheroidisation and the decay of less stable precipitates (e.g.  $M_3C$ ) to the favour of more stable particles (e.g.  $M_{23}C_6$  carbide) as well as precipitates of carbides rich in molybdenum ( $M_6C$ ). The detailed description

of precipitation processes taking place in Cr-Mo steels can be found, among other things, in publications [12, 14]. The identification of precipitates (performed using electron diffraction) revealed that the material subjected to the tests contained  $M_{23}C_6$  carbides along the boundaries of former austenite grains and along the boundaries of bainite laths as well as  $M_2C$  and  $M_{23}C_6$  carbides within the grains/laths (Fig. 3). The thermodynamic calculations performed using the TWC software programme revealed that, in relation to the test steel, the  $M_2C$  and  $M_{23}C_6$  carbides were equilibrium precipitants.

*Microstructure of the heat affected zone*

Depending on the distance from the heat source, the use of thermal energy during the welding process heats the material adjacent to the weld to various maximum temperatures, leading to the formation of the heat affected zone (HAZ). Primarily, the HAZ of the joint subjected to analysis (Fig. 4) contained two areas, i.e. a coarse-grained area and a normalised/partially normalised area. Near the fusion line, the material was characterised by the coarse-grained bainitic structure with single precipitates of various morphology present (similar to the base material) along the boundaries of former austenite grains as well as along and within bainite laths (Fig. 4). The effect of the high temperature of the welding cycle (significantly above  $A_{c3}$ ) led to the dissolution of the precipitates in the matrix. The decay (dissolution) of the precipitates precluded the impeding of the migration of grain boundaries, resulting in the growth of grain size and ultimately leading to the formation of the coarse-grained structure. The size of the grains of former austenite (determined by means of related patterns) in this area amounted to 6/5. As regards the normalised/partially normalised area, both the heating temperature affecting the area and the cooling

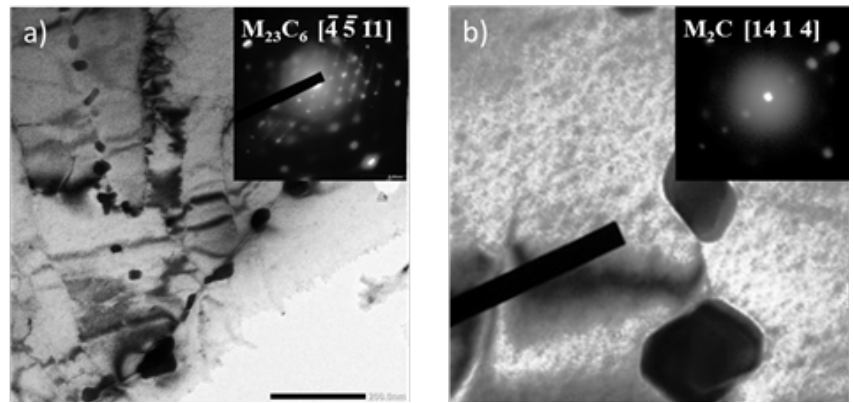


Fig. 3. Identification of precipitates in steel P5 after service: a)  $M_{23}C_6$  carbide along the grain boundary; b)  $M_2C$  carbide within the grain; TEM

rate were similar to the parameters of the normalising of steel.

As a result, in comparison with the base material, the foregoing led to the formation of the fine-grained microstructure (Fig. 5). The size of the former austenite grains (determined using related patterns) in this area amounted to 9/9, whereas the size of the grains in the base material amounted to 7/6. The aforesaid result was not only connected with the phase transformation but also with the only partial dissolution of the precipitates in the matrix. The foregoing precluded the grow of the grains and ultimately led to the maintaining of the fine-grained microstructure. The effect of the thermal cycle temperature in this area could not only be responsible for the dissolution of some precipitates but could also trigger the coagulation of undissolved precipitates. As a result, the area contained both large and small precipitates arranged in a similar manner as those located in the base material (Fig. 5). The coagulation of the precipitates in the area primarily concerned the  $M_{23}C_6$  carbides [11, 15], which was probably related to the faster diffusion of substitutive elements along the grain boundaries. According to information contained in publication [16, 17], in the welded joint of steel Cr-Mo, because of its fine-grained microstructure, the normalised/partially normalised area could develop creep damage (triggered by the IV type mechanism) during operation [18]. However, the authors of the publication also remarked that the fine-grained microstructure protected the

joints in steel Cr-Mo against brittleness connected with the segregation of trace elements along the grain boundaries. A similarly favourable effect of the fine-grained microstructure of steel Cr-Mo resulting in the reduction of the brittleness connected with the segregation of admixtures to grain boundaries was observed in publication [13].

*Microstructure of the weld*

The chemical composition of the filler metal (Table 5) corresponding to the base material (Table 4) and the cooling rate in the weld area determined the microstructure in this area of the joint. The weld was characterised by the coarse-grained bainitic or bainitic-martensitic structure with relatively few precipitates of various morphology arranged in a manner similar to the arrangement of the precipitates in the base material (Fig. 6). The solidification grains in the weld were elongated in the direction of heat discharge.

**Summary**

The element subjected to the above-presented tests discussed in the article was a section of a welded joint made of bainitic steel P5, (X11Cr-Mo5) after long-lasting exposure to elevated temperature. The tests revealed the relatively low exploitation degree of the test joint, which was manifested not only by the maintained bainitic microstructure but also but not very advanced precipitation processes. The relatively insignificant exhaustion of the test joint microstructure could be ascribed to the fact that the joint was subjected to relatively low temperature for a relatively short time.

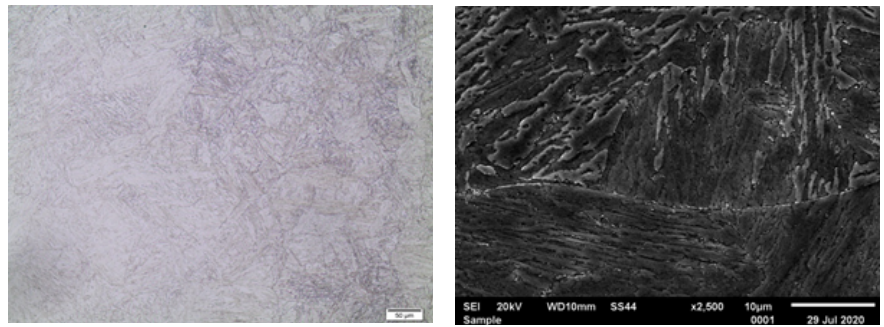


Fig. 4. Area near the fusion line of the test welded joint

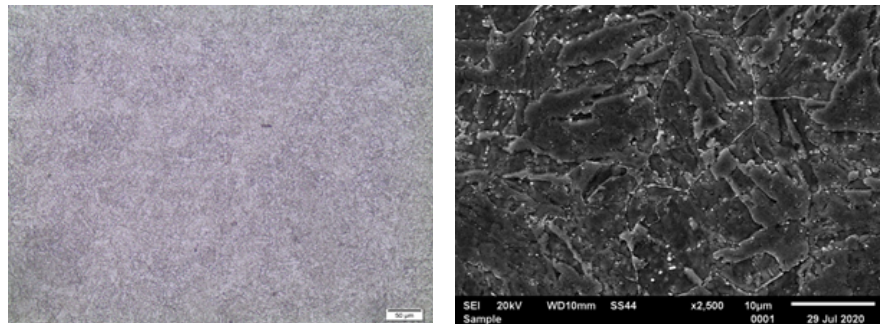


Fig. 5. HAZ of the test welded joint – visible fine-grained structure

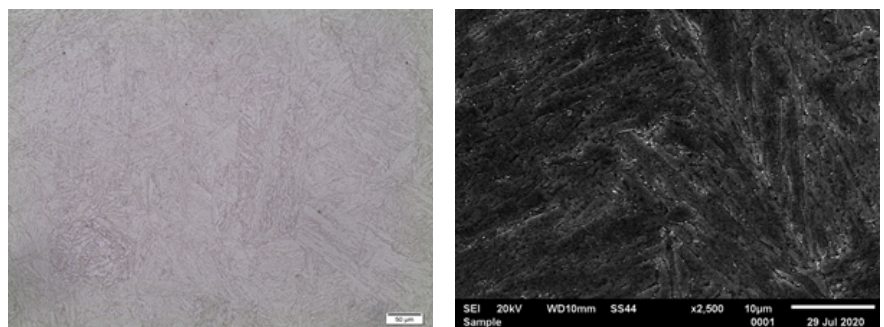


Fig. 6. Weld area in the test welded joint

**References**

[1] Golański G., Zieliński A., Słania J., Jasak J.: Mechanical properties of VM12 steel after 30 000 hrs of ageing at 600°C temperature. Archives of Metallurgy and Materials, 2014, vol. 59, no. 4, pp. 1357–1360.

[2] Zieliński A., Paszkowska H., Skupień P., Golański G.: Assessment of service life of HCM12 steel after 100 000 HRS of service. Archives of Metallurgy and Materials, 2016, vol. 61, pp. 1021–1029.

[3] Zeman M., Łomozik M., Brózda J.: Problems with welding steel T24 intended for membrane walls of boilers. Welding International, 2014, vol. 28, pp. 831–840.

[4] Golański G., Jasak J., Słania J.: Microstructure, properties and welding of T24 steel – critical review. Kovove

- Materialy-Metallic Materials, 2014, vol. 52, pp. 99–106.
- [5] Dobrzański J., Zieliński A., Paszkowska H.: Sposób oceny trwałości resztkowej na przykładzie materiału rodzimego i złącza spawanego po długotrwałej eksploatacji w warunkach pełzania znacznie poza czas obliczeniowy eksploatacji. Works of IMŻ 63/1, 2009, pp. 34–37.
- [6] Łomozik M., Zeman M., Jachym R.: Cracking of welded joints made of steel X10CrMoVNb9-1 (T91)—Case study. Kovove Materialy, 2012, vol. 50, no. 4, pp. 285–294.
- [7] Łomozik M., Hernas A., Zeman M.L.: Effect of welding thermal cycles on the structure and properties of simulated heat-affected zone areas in X10CrMoVNb9-1 (T91) steel at a state after 100,000 h of operation. Materials Science and Engineering: A 637, pp. 82–88.
- [8] Kumšlytis V., Skindaras R., Valiulis A. V.: The Structure and Properties of 5 % Cr-0.5 % Mo Steel Welded Joints after Natural Ageing and Post-weld Heat Treatment. Materials Science 18/2.
- [9] Material Data Sheet, Alloy steel tubes – P5 / T5, Peninsular Steel Tubes.
- [10] PN-EN ISO 5817:2014-05 – Spawanie – Złącza spawane ze stali, niklu, tytanu i ich stopów (z wyjątkiem spawanych wiązek) – Poziomy jakości według niezgodności spawalniczych
- [11] Saucedo-Muñoz M. L., Komazaki S. I., Avila-Davila E. O., Lopez-Hirata V. M., Dorantes-Rosales H. J.: Precipitation characterization and creep strength at 600°C for creep resistant Cr–Mo steel. ISIJ International, 2019.
- [12] Das S., Joarder A.: Effect of long-term service exposure at elevated temperature on microstructural changes of 5Cr-0.5Mo steels. Metallurgical and Materials Transactions A, 28, 1997, no. 8, pp. 1607–1616.
- [13] Zhao Y., Ma Q., Song S.: Hardening Embrittlement and Non-Hardening Embrittlement of Welding-Heat-Affected Zones in a Cr-Mo Low Alloy Steel. Metals, 2018, no. 8, pp. 1–12.
- [14] Wielgosz R.: Próba prognozowania trwałości stali chromowo-molibdenowych dla energetyki. Zeszyty Naukowe Politechniki Krakowskiej, 1988, no. 8.
- [15] Yu Z. S., Sun F., Zhanga J. X., Wang H. Z., Yuan Y., Zhao L., Liu X.: Effect of microstructural features on hardness in simulated heat affected zone of an advanced low-alloyed steel. Journal of Alloys and Compounds, 2017, vol. 697, pp. 86–89.
- [16] Khan S. A., Islam M. A.: Influence of prior austenite grain size on the degree of temper embrittlement in Cr-Mo steel. Journal of Materials Engineering and Performance, 2007, vol. 80, pp. 80–85.
- [17] Fujibayashi S., Endo T.: Creep behavior at the intercritical HAZ of a 1.25Cr-0.5Mo steel. ISIJ International, 2002, vol. 42, pp. 1309–1317.
- [18] Francis J. A., Mazur W., Bhadeshia H. K. D. H.: Review Type IV cracking in ferritic power plant steels. Materials Science and Technology, 2013, vol. 22, pp. 1387–1395.